Proc. Natl. Acad. Sci. USA
Vol. 90, pp. 6285–6289, July 1993
Neurobiology

Negatively charged amino acid residues in the nicotinic receptor δ subunit that contribute to the binding of acetylcholine

CYNTHIA CZAJKOWSKI*†, CHRISTINE KAUFMANN*, AND ARTHUR KARLIN*†‡§

*Center for Molecular Recognition and the Departments of †Biochemistry and Molecular Biophysics, ‡Physiology and Cellular Biophysics, and §Neurology, College of Physicians and Surgeons, Columbia University, New York, NY 10032

Communicated by Eric R. Kandel, April 15, 1993

ABSTRACT **In nicotinic receptors, the binding sites for acetylcholine are likely to contain negatively charged amino acid side chains that interact with the positively charged quaternary ammonium group of acetylcholine and of other potent agonists. We previously found that a 61-residue segment of the δ subunit contains aspartate or glutamate residues within 1 nm of cysteines in the acetylcholine binding site on the α subunit. We have now mutated, one at a time, the 12 aspartates and glutamates in this segment of the mouse muscle δ subunit and have expressed the mutant receptors in *Xenopus* oocytes. Both the concentration of acetylcholine eliciting half-maximal current (K_{app}) and the K_i for the inhibition by acetylcholine of α-bungarotoxin binding were increased 100-fold by the mutation of δAsp[180] to Asn and 10-fold by the mutation of δGlu[189] to Gln. These two residues, and their homologs in the γ and ε subunits, are likely to contribute to the acetylcholine binding sites.**

The binding of acetylcholine (ACh) by nicotinic receptors promotes channel opening and desensitization (1). It is axiomatic that these changes in functional state reflect changes in structure. On binding ACh, the structure of the binding site changes (2, 3). Because the ACh binding sites are extracellular and the gate is close to the cytoplasmic end of the channel (4), the local changes at the ACh binding sites are propagated to distant parts of the receptor. To understand the binding of ACh, the resulting local conformational changes, and the propagation of these changes, we need to identify the amino acid residues contributing to the binding of ACh and to locate these residues in the three-dimensional structure of the receptor.

Early work with affinity labels indicated that there is a readily reducible disulfide in the ACh binding site within 1 nm of the postulated negative subsite that binds the quaternary ammonium group of ACh and other potent agonists and competitive antagonists (5). This disulfide is formed by adjacent cysteines, αCys[192] and αCys[193], on the α subunit (6, 7). A number of other α-subunit residues, all aromatic, have also been identified by ACh-binding-site-directed labeling. These are αTyr[93] (8, 9), αTrp[149] (10), αTyr[190] (10, 11), and αTyr[198] (12) (Fig. 1). Their involvement in ACh binding was further supported by the functional consequences of their alteration by site-directed mutagenesis (22–25). These cysteines and aromatic residues are completely conserved in all known α-subunit sequences.

Aspartate and glutamate residues, which would be the obvious candidates for the postulated negative subsite, were not among the residues identified as contributing to the ACh binding site, and it is possible that they are not required. The affinity label, acetylcholine mustard, which is capable of reacting with carboxylates, labeled only αTyr[93] (9). Others have suggested that the quaternary ammonium group could

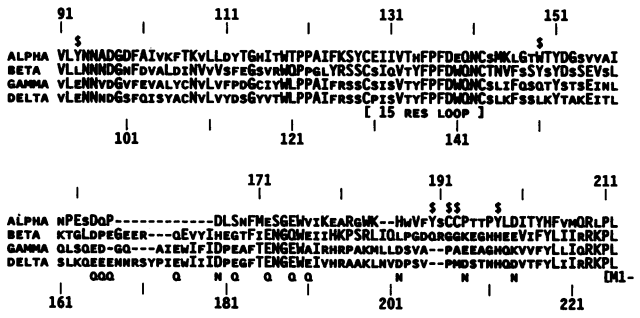

FIG. 1. Aligned subsequences of mouse α, β, γ, and δ subunits. Residues in α that were previously identified (see text) as contributing to the ACh binding site are marked with $. The mutations in δ reported here are shown below the wild-type residues. In the α sequence, the large type represents residues that are identical in the aligned sequences of human, bovine, and *Torpedo* (13), mouse (14), and *Xenopus* (15) α subunits. In the β sequence, the large type represents residues identical in human (16), mouse (17), *Torpedo* (13), and bovine (13) β subunits. In the γ and δ sequences, large type represents residues that are identical in human (13), bovine (13), *Torpedo* (13), mouse (18), chicken (19), and *Xenopus* (15) γ subunits; in bovine (13), *Torpedo* (13), mouse (20), chicken (19), and *Xenopus* (15) δ subunits; and in bovine (13) and rat (21) ε subunits. The numbering is for the processed chains: the top numbers are for α and the bottom numbers are for δ. Like the α subsequence, the β and γ subsequences start at residue 91, and δ starts at residue 93. "[M1-" marks the beginning of the first membrane-spanning segment.

be bound by the electron-rich aromatic rings of tyrosine, tryptophan, and phenylalanine (26) or by ionized tyrosine phenolate side chains (8).

There are, however, aspartates or glutamates in the receptor close enough to αCys[192]/Cys[193] to contribute to the binding of ACh. Using a crosslinker that reacts specifically with sulfhydryls at one end and with carboxyl groups at the other end, we found in *Torpedo* ACh receptor that there are aspartate or glutamate residues on the δ subunit within 0.9 nm of αCys[192] and αCys[193] (27). The crosslinked aspartate or glutamate residues are located within a segment, aa δ164–224, containing six aspartates and five glutamates. We have now used site-directed mutagenesis and expression in *Xenopus* oocytes as a parallel approach to identifying which of these aspartates and glutamates might contribute to ACh binding. For this we turned to the mouse muscle receptor, because it has a longer mean open time and gives larger currents when expressed in *Xenopus* oocytes than does the *Torpedo* receptor (28, 29). The segment of mouse muscle δ that aligns with *Torpedo* aa δ164–224 contains four aspartates and eight glutamates (Fig. 1). Eight of these 12 mouse residues are conserved in *Torpedo*. We determined the functional consequences of mutating each of the 12 aspartates and glutamates to asparagine and glutamine, respectively. We expected that if a side-chain carboxylate of an aspartate

The publication costs of this article were defrayed in part by page charge payment. This article must therefore be hereby marked "*advertisement*" in accordance with 18 U.S.C. §1734 solely to indicate this fact.

Abbreviation: ACh, acetylcholine.

or glutamate did interact directly with ACh, then mutation of such a residue to an asparagine or glutamine would markedly weaken the binding of ACh.

MATERIALS AND METHODS

Mouse muscle ACh receptor subunit cDNAs (provided by T. Claudio, Yale University) were subcloned into pSP64T at the *Bgl* II site. We generated a mutagenesis cassette for the δ subunit by eliminating the *Ava* I site in the multiple cloning site of δ-pSP64T by cutting with *Sma* I and ligating in a *Not* I linker; this made the *Ava* I site in the δ cDNA unique. We carried out mutagenesis on the δ subunit in a cassette defined by the restriction enzymes *Ava* I and *Kpn* I (30, 31). The mutant cassettes were sequenced in both directions. Capped mRNA for each subunit was generated with SP6 RNA polymerase under standard conditions (Promega) from the cDNA in the pSP64T plasmid.

Oocytes from *Xenopus laevis* were prepared by incubating small pieces of ovary in collagenase (20 mg/ml; Sigma type I) in OR3 medium [1:2 dilution of Lebovitz L-15 medium/1 mM glutamine/gentamicin (100 μg/ml)/15 mM Hepes, pH 7.6 with NaOH] for 20 min at 17°C (32). The pieces were washed five times in OR3, and the oocytes were dissected. One day later, the oocytes were injected with 50 nl of total mRNA (200 pg/nl), consisting of mRNAs for the subunits in the ratios 2:1:1:1 for the combination αβγδ, the ratios 2:1:2 for the combination αβγ, the ratios 2:1:4 for αβδ, and the ratio 2:1 for αβ. Oocytes were used for electrophysiological experiments or for preparing membrane homogenates 2–6 days after being injected.

ACh-induced currents were recorded with a two-electrode voltage clamp at a holding potential of −40 mV. Electrodes were filled with 3 M KCl and had a resistance of <2 MΩ. The oocytes were held in a narrow trough and perfused at 5 ml/min (velocity, ≈4 cm/s) with Ca-free Ringers solution (115 mM NaCl/2.5 mM KCl/1.8 mM $MgCl_2$/0.001 mM atropine/10 mM Hepes, pH 7.5 with NaOH), in which all reagents were applied.

Oocyte membranes were prepared by homogenizing 100–200 injected oocytes in a Dounce homogenizer in 10–20 ml of ice-cold homogenization buffer (83 mM NaCl/1 mM $MgCl_2$/10 mM Hepes/5 mM EDTA/5 mM EGTA/1 mM phenylmethylsulfonyl fluoride, pH 7.9) (33). Homogenates were centrifuged for 10 min at 800 × *g*, the supernatants were saved, and the pellets were suspended in buffer and pelleted. The combined supernatants (≈42 ml) were divided, and each half was layered over 4 ml of 15% (wt/vol) sucrose and centrifuged at 4°C in a Beckman Ti 50.2 rotor at 50,000 rpm for 1.2 hr. The pellets were suspended in NP50 buffer (50 mM NaCl/10 mM sodium phosphate/1 mM EDTA, pH 7.1) at 5 μl per oocyte and stored in liquid nitrogen. Protein was assayed using bovine serum albumin as a standard (34). The final membrane suspension contained ≈2.6 μg of protein per μl. The yield was ≈10 fmol of toxin binding sites and 13 μg of protein per oocyte.

The affinity for ^{125}I-labeled α-bungarotoxin (^{125}I-labeled toxin) was determined by diluting 25–50 μl of membrane suspension to 400 μl with NP50 containing 0.2% Triton X-100, mixing with ^{125}I-labeled toxin (at seven concentrations from 0.03 nM to 3 nM), and holding at 18°C overnight. The samples were then diluted with 5 ml of ice-cold wash buffer (0.2% Triton X-100/10 mM NaCl/10 mM sodium phosphate, pH 7.4), filtered through two DE81 filters, and washed three times. The amount of ^{125}I-labeled toxin on the filters was determined by liquid scintillation counting. Nonspecific binding was determined in the presence of 1 μM unlabeled α-bungarotoxin.

The equilibrium dissociation constant for ACh was determined from its inhibition of ^{125}I-labeled toxin binding. Membrane was incubated for 20 min with 200 μM diisopropyl phosphofluoridate to inactivate acetylcholinesterase. Membrane (5–20 μl), 0.25 nM ^{125}I-labeled toxin, and various concentrations of ACh, all in NP50, were combined in a final volume of 300 μl. After 5 hr at room temperature, the suspension was filtered, and the bound ^{125}I-labeled toxin was determined as above. Toxin binding reached equilibrium within 5 hr.

RESULTS

To assess the possible involvement of side-chain carboxylate groups in the binding of ACh, we mutated each aspartate and glutamate in mouse muscle aa δ164–224 to its uncharged amidated counterpart (Fig. 1). We expressed the mutant δ subunit with wild-type subunits, either α and β or α, β, and γ. For each combination, we recorded the ACh-induced current at five to seven ACh concentrations (Fig. 2).

Three of the 12 mutant δ subunits, when expressed with wild-type α and β, were characterized by K_{app} values that were 10-fold or more greater than the K_{app} value for wild-type αβδ (Table 1). The mutant δD180N was characterized by a K_{app} of 227 μM, 84 times larger than the K_{app} of 2.7 μM for wild-type αβδ (Fig. 2 and Table 1). The K_{app} of δE189Q was 13 times larger than wild type, and the K_{app} of δD214N was 11 times larger. In the remaining 9 mutants, the increase in K_{app} was 3-fold or less (Table 1). The three mutants with the largest increases in K_{app} had peak currents that were 30–74% of the peak current for wild-type αβδ. The increases in K_{app}, however, are not correlated with a reduction in peak current: for example, the peak current of the mutant δE186Q was 43% of wild-type αβδ, but the change in K_{app} was insignificant.

When δD180N or δE189Q was expressed with wild-type α, β, and γ subunits, the K_{app} values were <2-fold greater than the K_{app} of wild-type αβγδ. We could not be certain, however, that the mutant δ subunits were included in all functional receptor complexes on the oocyte surface. When we omitted δ and injected just wild-type α, β, and γ, we also obtained a K_{app} <2-fold greater than that of αβγδ (Table 1; cf. refs. 35 and 36). In contrast, the response of oocytes expressing mutant δ and wild-type α and β, in the absence of γ,

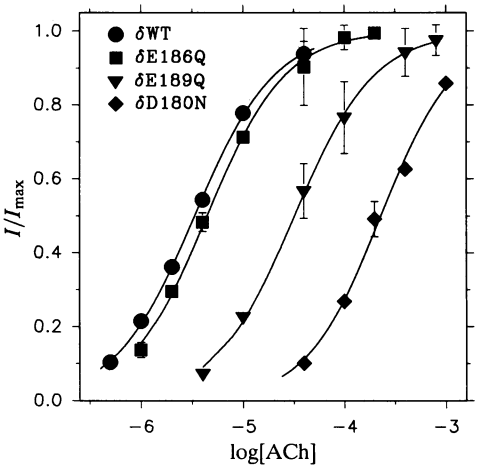

FIG. 2. Dose–response curves for receptors composed of mouse muscle α, β, and δ subunits expressed in *Xenopus* oocytes. The α and β subunits were wild type, and δ subunits were wild type (circles) or the mutants E186Q (squares), E189Q (triangles), or D180N (diamonds). ACh at the indicated concentrations was added for 10 s, and the peak current, at a holding potential of −40 mV, was recorded. Each concentration was added twice, and the peak currents (*I*) were averaged. These are shown divided by the maximal current (I_{max}), calculated by fitting the Hill equation to the data (see Table 1); the fitted curves are shown. Each curve is from a single oocyte.

Table 1. Characteristics of the ACh-induced currents in voltage-clamped *Xenopus* oocytes expressing mutant δ subunits and wild-type α, β, and γ subunits

Subunits injected	Mutation	K_{app}, μM	$K_{app}/K_{app}\alpha\beta\delta$	I_{max}, nA	*n*
αβγδ	None	2.6 ± 0.4	1.0 ± 0.2	3165 ± 171	12
αβγ	None	4.4 ± 0.9	1.6 ± 0.4	3079 ± 127	3
αβδ	None	2.7 ± 0.3	1	1808 ± 276	7
αβ	None	NDR	NDR		9
αβγδ	D180N	5.1 ± 0.8	1.9 ± 0.4	3775 ± 743	2
αβγδ	E186Q	3.1 ± 1.4	1.1 ± 0.5	3342 ± 341	2
αβγδ	E189Q	2.5 ± 0.3	0.9 ± 0.2	3339 ± 373	3
αβδ	E165Q	6.3 ± 1.0	2.3 ± 0.4	1839 ± 300	3
αβδ	E166Q	2.7 ± 0.5	1.0 ± 0.2	1458 ± 175	3
αβδ	E167Q	5.2 ± 1.2	1.9 ± 0.5	1004 ± 279	4
αβδ	E175Q	5.0 ± 0.6	1.8 ± 0.3	1716 ± 177	8
αβδ	D180N	227 ± 26	84 ± 13	693 ± 109	9
αβδ	E182Q	8.9 ± 1.0	3.3 ± 0.5	1439 ± 69	7
αβδ	E186Q	5.6 ± 1.1	2.1 ± 0.5	776 ± 323	6
αβδ	E189Q	36 ± 4	13 ± 2	1342 ± 110	8
αβδ	E191Q	7.8 ± 1.3	2.9 ± 0.6	1962 ± 142	5
αβδ	D202N	2.3 ± 0.5	0.8 ± 0.2	1612 ± 644	3
αβδ	D208N	3.8 ± 0.5	1.4 ± 0.2	1059 ± 294	3
αβδ	D214N	31 ± 6	11 ± 2	537 ± 80	5

Oocytes were injected with subunit mRNA and tested. Ten-second pulses of ACh were separated by 5-min washes with Ca-free Ringer's solution. Each oocyte was exposed to five to seven concentrations of ACh, usually in duplicate. The peak currents (at a −40 mV holding potential) were fit to the Hill equation, $I = I_{max}/(1 + (K_{app}/[ACh])^{n_H})$, using the Marquardt–Levenberg nonlinear least-squares algorithm. n_H varied from 0.84 to 1.64. The means ± SEM of the parameters are shown. The mutations are indicated as XnX', where X is the wild-type residue, n is its position in the δ sequence, and X' is the substituted residue. The number of experiments (*n*) is given. NDR, no detectable response.

was certainly due to receptor complexes containing the mutant δ, because the combination of α and β did not yield a detectable response to ACh (Table 1). The K_{app} for wild-type αβδ did not differ from that for αβγδ (Table 1); the receptor composed of mouse α, β, and δ and the receptor composed of mouse α, β, γ, and δ have the same functional properties (36–38). Thus, we assessed the effects of mutation of δ in the γ-less complex.

None of the mutations, δD180N, δE186Q, δE189Q, or δD214N, had a significant effect on the equilibrium dissociation constant for the binding of ^{125}I-labeled toxin (Table 2). Tomaselli *et al.* (23) found that mutations of other residues likely to interact with ACh, αTyr^{190} and αTyr^{198}, also did not affect toxin binding. In contrast, the ability of ACh to compete with ^{125}I-labeled toxin was very impaired in δD180N: the K_i for ACh was 190-fold greater than that of wild-type αβδ (Fig. 3 and Table 2). In the mutant δE189Q, the K_i for ACh was ≈6 times the K_i for wild type. For these two mutants, the changes in K_i were in the same direction and of similar magnitude to the changes in K_{app}. In the mutant δD214N, however, the K_i was ≈50% the K_i of wild type; the K_{app}, however, was 11 times larger than that of wild type; the effects of the mutation on K_i and on K_{app} were in opposite directions.

Not all of the specific binding of toxin could be inhibited by ACh. At a saturating concentration of ACh, 50–82% of the specific toxin binding was inhibited (Table 2). Toxin binding was determined in a crude membrane fraction of oocytes that included both surface and intracellular membranes. The binding of toxin to unassembled α in intracellular membranes may account for the portion of toxin binding to oocyte membranes not blockable by ACh (39, 40). In oocytes injected with α, β, and δ, the fraction of the toxin binding that could be inhibited by ACh was due to binding to receptor complexes containing the δ subunit, because toxin binding to membranes from oocytes injected with only α and β was not inhibited by ACh (Table 2).

DISCUSSION

Based on our results above, δAsp^{180} and δGlu^{189} are likely contributors to the negative subsite of the ACh binding site. We assumed that if a side-chain carboxylate of an aspartate or a glutamate did interact directly with ACh, then mutation of such a residue to an asparagine or a glutamine would markedly weaken the binding of ACh. Thus, if a mutation had little effect on ACh binding, we could eliminate the mutated aspartate or glutamate as an important contributor to the negative subsite. Mutation of 9 of the 12 aspartates and glutamates in aa δ164–224 had little or no effect on ACh binding. In contrast, the mutation of three residues, δAsp^{180}, δGlu^{189}, and δAsp^{214}, led to a 10-fold or greater increase in K_{app} (Table 1). For two of these residues, δAsp^{180} and δGlu^{189}, the effects of mutation on K_i was consistent with the effects on K_{app} (Tables 1 and 2). For δAsp^{214}, the effects on K_{app} and K_i were in opposite directions.

Both K_{app} and K_i depend on local interactions of ACh with residues in the binding site and on nonlocal conformational changes in the receptor linked to the binding. Channel gating and desensitization are manifestations of nonlocal changes, and changes in the kinetics of these processes could alter the K_{app} or K_i (e.g., ref. 36). The opposite effects of mutation of δAsp^{214} on K_{app} and K_i suggest that these effects are not on the local interactions of ACh, but rather on the kinetics of nonlocal processes. In contrast, the similarity of the effects on K_{app} and K_i of the mutations of δAsp^{180} and of δGlu^{189} are

Table 2. Binding of ^{125}I-labeled α-bungarotoxin and of acetylcholine to membranes of *Xenopus* oocytes expressing mutant δ subunits

Subunits injected	Mutation	K_x (toxin), pM	Y_{max} (toxin), fmol per oocyte	K_i (ACh), μM	$K_i/K_i\alpha\beta\delta$	Maximum block by ACh, %
αβγδ	None	1150 ± 600 (2)	11 ± 4	0.24 ± 0.04 (3)	2.8 ± 1.0	77 ± 2
αβδ	None	520 ± 130 (3)	4.2 ± 0.9	0.087 ± 0.029 (3)	1	69 ± 12
αβ	None	ND	2.4 ± 0.2*	No block (3)		0
αβδ	D180N	420 ± 110 (3)	4.0 ± 0.6	16.6 ± 6.7 (3)	190 ± 99	56 ± 3
αβδ	E186Q	330 ± 60 (3)	3.1 ± 0.5	0.11 ± 0.04 (2)	1.3 ± 0.6	65 ± 18
αβδ	E189Q	800 ± 410 (3)	5.0 ± 1.8	0.57 ± 0.15 (4)	6.5 ± 2.8	50 ± 3
αβδ	D214N	380 ± 70 (2)	3.0 ± 0.2	0.049 ± 0.022 (2)	0.6 ± 0.3	82 ± 7

K_x and Y_{max} values for ^{125}I-labeled toxin were calculated by a nonlinear least-squares fit of the specifically bound toxin, *Y*, to the equation, $Y = Y_{max}/(1 + K_x/X)$, where *X* is the ^{125}I-labeled toxin concentration. K_i for ACh and the ^{125}I-labeled toxin binding not blockable by ACh (*U*) were calculated by a nonlinear least-squares fit of the specifically bound toxin, *Y*, to the equation, $Y = (Y_0 - U)/[1 + (A/K_i)/(1 + X/K_x)] + U$, where Y_0 is ^{125}I-labeled toxin specifically bound in the absence of ACh, *A* is the concentration of ACh, *X* is the concentration of ^{125}I-labeled toxin (0.25 nM), and K_x is the equilibrium dissociation binding constant of ^{125}I-labeled toxin. The means ± SEM of the parameters and the number of experiments (in parentheses) are shown. ND, not determined.

*Y_{max} was estimated in this case from the binding at 0.25 nM ^{125}I-labeled toxin and the assumption that K_x was 0.5 nM.

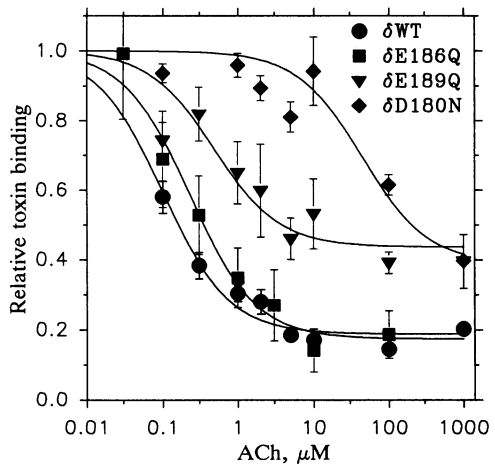

FIG. 3. Inhibition by ACh of ^{125}I-labeled α-bungarotoxin binding to membranes from *Xenopus* oocytes expressing mouse muscle α, β, and δ subunits. The α and β subunits were wild type, and δ subunits were wild type (circles) or the mutants E186Q (squares), E189Q (triangles), or D180N (diamonds). The quantity of toxin specifically bound at each ACh concentration was divided by the quantity specifically bound in the absence of ACh. Each curve is from a single experiment, and each point is the mean of triplicate determinations. The curves were fitted to the data as in Table 2.

consistent with effects on the local interactions of ACh with its binding site. Also, comparison of the magnitude of the effects of the mutation δD180N (100-fold) and the magnitude (≈10) of the gating isomerization constant (36, 41) suggests that the mutation δD180N does significantly affect the local interactions of ACh. Nevertheless, an effect on the local interactions at the binding site does not prove that the mutated residue is in the site. The location of δAsp^{180} and/or δGlu^{189} within the binding site is supported by the finding that they are among 12 carboxylate residues in aa δ164–224, one or more of which is within 0.9 nm of αCys^{192}/Cys^{193} (27).

The receptor has two nonidentical ACh binding sites (42–44). In the native receptor, with composition $\alpha_2\beta\gamma\delta$ (45), one site is formed between the first α subunit and the δ subunit, and the other site is formed between the second α subunit and the γ subunit (39, 40, 46). Furthermore, ε substitutes for γ in adult muscle ACh receptor (47) and also must form an ACh binding site with α. In aa δ164–224, only three carboxylate residues, δAsp^{180}, δGlu^{186}, and δGlu^{189}, are conserved among all aligned segments of δ, γ, and ε subunits (Fig. 1). The pattern of conservation of δAsp^{180} and δGlu^{189} is consistent with their role in the ACh binding site formed between α and δ and with the identical roles of these residues in γ, δ, and ε. In contrast, in all the aligned β-subunit sequences, histidine or asparagine aligns with δAsp^{180} and glutamine aligns with δGlu^{189} (Fig. 1). The combination of α and β forms an ACh binding site poorly (39, 40, 48). This could be due to the absence of residues in β corresponding to δAsp^{180} and δGlu^{189} and/or to the poor assembly of α and β in the absence of other subunits. δAsp^{180} and δGlu^{189} are conserved in α, but muscle-type α does not form a homo-oligomer and does not form an ACh binding site (40, 49).

In a speculative model of the ACh binding sites, we place one site between α and δ and another between α and γ (Fig. 4). The residues that have been identified as possible contributors to ACh binding (αTyr^{93}, αTrp^{149}, αTyr^{190}, αCys^{192}, αCys^{193}, and αTyr^{198}; δAsp^{180}, and δGlu^{189}; and the aligned γAsp^{174} and γGlu^{183}) are arrayed around the binding sites. The residues aligned (Fig. 1) with these binding-site residues in all subunits are also displayed. The location of residues is constrained by the quasi-fivefold symmetry of the subunits around the channel axis (50), by the order of the subunits

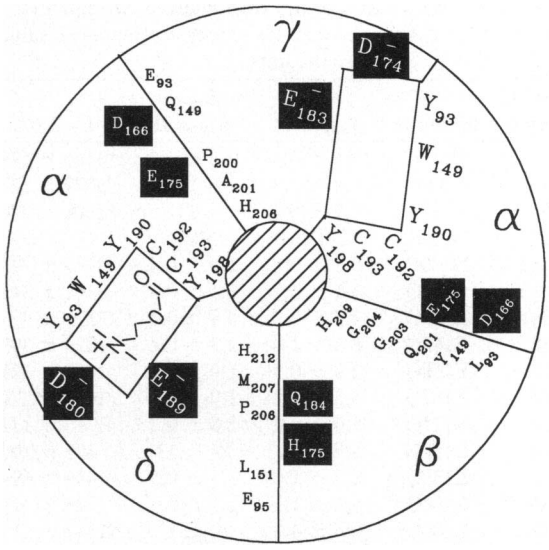

FIG. 4. Speculative model of the ACh binding sites of the nicotinic ACh receptor. The receptor is schematically represented in top view, with the subunits surrounding the central channel. The ACh binding sites are represented by rectangles between α and δ and between α and γ subunits. Around the rectangles are all the residues implicated in the binding of ACh. All residues are from the mouse muscle sequences (Fig. 1). Residues that are likely to contribute to the negative subsites, δAsp^{180} and δGlu^{189} or γAsp^{174} and γGlu^{183}, are shown in reverse contrast, as are the aligned residues in the other subunits. By symmetry, all these residues will be on the same (clockwise) side of their subunits. The residues in α that contribute to the binding site (αTyr^{93}, αTrp^{149}, αTyr^{190}, αCys^{192}, αCys^{193}, and αTyr^{198}) and the aligned residues in the other subunits are at the counterclockwise side of their subunits. ACh is shown bound to the α–δ site, which is contracted compared to the unliganded α–γ site. The contraction of the site across the subunit–subunit interface is postulated to shift the one subunit relative to the other. This structural change is transmitted across the membrane to the channel gate.

around the channel (51), and by the similar tertiary structures of the subunits (52). Corresponding residues in the aligned sequences of the subunits (Fig. 1) must occupy nearly identical positions in the folded structures of each of the subunits and must be superimposable by a multiple of a 72° rotation around the channel axis (Fig. 4). In keeping with fivefold symmetry, δAsp^{180} and δGlu^{189} are shown on the clockwise side of δ, and their homologs, γAsp^{174} and γGlu^{183}, are shown on the clockwise side of γ. Likewise, the aligned residues in α and β are shown on the clockwise side of these subunits. (Residues on the clockwise side of each subunit are shown in reverse contrast.) Conversely, αTyr^{93}, αTrp^{149}, αTyr^{190}, αCys^{192}, αCys^{193}, and αTyr^{198} are on the counterclockwise side of α. These residues can participate in the binding of ACh only if they are at the same surface of α—i.e., the surface that forms an interface with γ or δ. By symmetry and the similar tertiary structure of the subunits, the residues in β, γ, and δ that align with the binding-site residues in α are on the counterclockwise sides of these subunits. The sets of residues at the three-subunit interfaces that do not form ACh binding sites are quite different from the sets of residues at the α–δ and α–γ interfaces that do form binding sites (Fig. 4).

Because of the symmetry and similar tertiary structure of the subunits, residues in two subunits that are aligned in the sequences cannot be juxtaposed at the same interface between the subunits. For example, δAsp^{214} is aligned with a residue in α 2 residues away from αTyr^{198} (Fig. 1), and therefore, δAsp^{214} and αTyr^{198} cannot be at the same subunit–subunit interface. δAsp^{214} cannot be in the ACh binding site if αTyr^{198} is there, further supporting our conclusion above that the mutation of δAsp^{214} has a nonlocal effect on binding.

Conversely, δGlu[189] is aligned with a residue in α that is 15 residues away from αTyr[190] (Fig. 1). Fifteen residents could span from one side of a subunit to the other (Fig. 4). (The diameter of the receptor is about 8 nm, and the distance across a subunit midway between the channel and the outer circumference is ≈2.5 nm.) Therefore, δGlu[189] and αTyr[190] could be on different sides of their subunits and juxtaposed at the interface between the subunits; these residues could contribute to the same binding site (Fig. 4).

As in this model of the ACh binding sites, the binding site for the quaternary ammonium group of phosphocholine in an anti-phosphocholine antibody is formed by aspartate, glutamate, and aromatic residues (53, 54). In the antibody, as in the receptor, the binding site is formed by residues from two polypeptide chains. Furthermore, the binding of ACh at the catalytic site of acetylcholinesterase likely involves interaction with aromatic residues (55) and with at least one glutamate residue (56).

Previously, it was inferred that ACh and other agonists bridge the binding site, from the negative subsite, which binds the quaternary ammonium group, to the region around the disulfide, which binds the acetyl group, promoting a decrease in the distance between these two ends of the binding site (ref. 5 and Fig. 4). Because the disulfide is on the α subunit (6, 7, 57) and δAsp[180] and δGlu[189], which we hypothesize contribute to the negative subsite, are on a neighboring subunit, this contraction of the binding site could be immediately translated into a movement of one subunit relative to another. This movement of the subunits could be readily propagated to the channel gate (see ref. 50), which is close to the cytoplasmic side of the membrane (4).

We thank M. Akabas, P. Brehm, T. Claudio, J. Javitch, I. Lowy, M. Martin, L. Role, and D. Stauffer for invaluable advice and materials, and G. Salazar-Jimenez for technical assistance. This research was supported in part by research grants from the National Institutes of Health (NS07065) and from the Muscular Dystrophy Association, Inc. C.C. was partially supported by National Institutes of Health Training Grant NS07258.

1. Katz, B. & Thesleff, S. (1957) *J. Physiol. (London)* **138**, 63–80.
2. Damle, V. N. & Karlin, A. (1980) *Biochemistry* **19**, 3924–3932.
3. Galzi, J.-L., Revah, F., Bouet, F., Menez, A., Goeldner, M., Hirth, C. & Changeux, J.-P. (1991) *Proc. Natl. Acad. Sci. USA* **88**, 5051–5055.
4. Akabas, M. H., Stauffer, D. A., Xu, M. & Karlin, A. (1992) *Science* **258**, 307–310.
5. Karlin, A. (1969) *J. Gen. Physiol.* **54**, 245s–264s.
6. Kao, P. N., Dwork, A. J., Kaldany, R.-R. J., Silver, M. L., Wideman, J., Stein, S. & Karlin, A. (1984) *J. Biol. Chem.* **259**, 11662–11665.
7. Kao, P. N. & Karlin, A. (1986) *J. Biol. Chem.* **261**, 8085–8088.
8. Galzi, J.-L., Revah, F., Black, D., Goeldner, M., Hirth, C. & Changeux, J.-P. (1990) *J. Biol. Chem.* **265**, 10430–10437.
9. Cohen, J. B., Sharp, S. D. & Liu, W. S. (1991) *J. Biol. Chem.* **266**, 23354–23364.
10. Dennis, M., Giraudat, J., Kotzyba-Hibert, F., Goeldner, M., Hirth, C., Chang, J.-Y., Lazure, C., Chretien, M. & Changeux, J.-P. (1988) *Biochemistry* **27**, 2346–2357.
11. Abramson, S. N., Li, Y., Culver, P. & Taylor, P. (1989) *J. Biol. Chem.* **264**, 12666–12672.
12. Middleton, R. E. & Cohen, J. B. (1991) *Biochemistry* **30**, 6987–6997.
13. Numa, S. (1989) *Harvey Lect.* **83**, 121–165.
14. Isenberg, K. E., Mudd, J., Shah, V. & Merlie, J. P. (1986) *Nucleic Acids Res.* **14**, 5111.
15. Baldwin, T. J., Yoshihara, C. M., Blackmer, K., Kintner, C. R. & Burden, S. K. (1988) *J. Cell Biol.* **106**, 469–478.
16. Beeson, D., Brydson, M. & Newson-Davis, J. (1989) *Nucleic Acids Res.* **17**, 4391.
17. Buonanno, A., Muss, J., Shah, V. & Merlie, J. P. (1986) *J. Biol. Chem.* **261**, 16451–16458.
18. Yu, L., LaPolla, R. J. & Davidson, N. (1986) *Nucleic Acids Res.* **14**, 3539–3555.
19. Nef, P., Mauron, A., Stalder, R., Alliod, C. & Ballivet, M. (1984) *Proc. Natl. Acad. Sci. USA* **81**, 7975–7979.
20. LaPolla, R. J., Mayne, K. M. & Davidson, N. (1984) *Proc. Natl. Acad. Sci. USA* **81**, 7970–7974.
21. Criado, M., Witzemann, V., Koene, M. & Sakmann, B. (1988) *Nucleic Acids Res.* **16**, 10920.
22. Mishina, M., Tobimatsu, T., Imoto, K., Tanaka, K., Fujita, Y., Fukuda, K., Kurasaki, M., Takahashi, H., Morimoto, Y., Hirose, T., Inayama, S., Takahashi, T., Kuno, M. & Numa, S. (1985) *Nature (London)* **313**, 364–369.
23. Tomaselli, G. F., McLaughlin, J. T., Jurman, M. E., Hawrot, E. & Yellen, G. (1991) *Biophys. J.* **60**, 721–727.
24. Galzi, J.-L., Bertrand, D., Devillers-Thiery, A., Revah, F., Bertrand, S. & Changeux, J.-P. (1991) *FEBS Lett.* **294**, 198–202.
25. O'Leary, M. E. & White, M. M. (1992) *J. Biol. Chem.* **267**, 8360–8365.
26. Dougherty, D. A. & Stauffer, D. A. (1990) *Science* **250**, 1558–1560.
27. Czajkowski, C. & Karlin, A. (1991) *J. Biol. Chem.* **266**, 22603–22612.
28. Yoshii, K., Yu, L., Mayne, K. M., Davidson, N. & Lester, H. A. (1987) *J. Gen. Physiol.* **90**, 553–573.
29. Yu, L., Leonard, R. J., Davidson, N. & Lester, H. A. (1991) *Mol. Brain Res.* **10**, 203–211.
30. Nelson, R. M. & Long, G. L. (1989) *Anal. Biochem.* **180**, 147–151.
31. Kuipers, O. P., Boot, H. J. & de Vos, W. M. (1991) *Nucleic Acids Res.* **19**, 4558.
32. Camacho, P., Liu, Y., Mandel, G. & Brehm, P. (1993) *J. Neurosci.* **13**, 605–613.
33. Pradier, L., Yee, A. S. & McNamee, M. G. (1989) *Biochemistry* **28**, 6562–6571.
34. Lowry, O. H., Rosebrough, N. J., Farr, A. L. & Randall, R. J. (1951) *J. Biol. Chem.* **193**, 265–275.
35. Kullberg, R., Owens, J. L., Camacho, P. & Brehm, P. (1990) *Proc. Natl. Acad. Sci. USA* **87**, 2067–2071.
36. Sine, S. M. & Claudio, T. (1991) *J. Biol. Chem.* **266**, 19369–19377.
37. Lo, D. C., Pinkham, J. L. & Stevens, C. F. (1990) *Neuron* **5**, 857–866.
38. Charnet, P., Labarca, C. & Lester, H. (1992) *Mol. Pharmacol.* **41**, 708–717.
39. Kurosaki, T., Fukuda, K., Konno, T., Mori, Y., Tanaka, K., Mishina, M. & Numa, S. (1987) *FEBS Lett.* **214**, 253–258.
40. Blount, P. & Merlie, J. P. (1989) *Neuron* **3**, 349–357.
41. Steinbach, J. H. (1989) *Annu. Rev. Physiol.* **51**, 353–365.
42. Damle, V. N. & Karlin, A. (1978) *Biochemistry* **17**, 2039–2045.
43. Neubig, R. R. & Cohen, J. B. (1979) *Biochemistry* **18**, 5464–5475.
44. Dowding, A. J. & Hall, Z. W. (1987) *Biochemistry* **26**, 6372–6381.
45. Reynolds, J. A. & Karlin, A. (1978) *Biochemistry* **17**, 2035–2038.
46. Pedersen, S. E. & Cohen, J. B. (1990) *Proc. Natl. Acad. Sci. USA* **87**, 2785–2789.
47. Mishina, M., Takai, T., Imoto, K., Noda, M., Takahashi, T., Numa, S., Methfessel, C. & Sakmann, B. (1986) *Nature (London)* **321**, 406–411.
48. Golino, M. D. & Hamill, O. P. (1992) *J. Membr. Biol.* **129**, 297–309.
49. Blount, P. & Merlie, J. P. (1988) *J. Biol. Chem.* **263**, 1072–1080.
50. Unwin, N. (1989) *Neuron* **3**, 65–76.
51. Karlin, A., Holtzman, E., Yodh, N., Lobel, P., Wall, J. & Hainfeld, J. (1983) *J. Biol. Chem.* **258**, 6678–6681.
52. Noda, M., Takahashi, H., Tanabe, T., Toyosato, M., Kikyotani, S., Furutani, Y., Hirose, T., Takashima, H., Inayama, S., Miyata, T. & Numa, S. (1983) *Nature (London)* **302**, 528–532.
53. Satow, Y., Cohen, G. H., Padlan, E. A. & Davies, D. R. (1986) *J. Mol. Biol.* **190**, 593–604.
54. Glockshuber, R., Stadlmuller, J. & Pluckthun, A. (1991) *Biochemistry* **30**, 3049–3054.
55. Sussman, J. L., Harel, M., Frolow, F., Oefner, C., Goldman, A., Toker, L. & Silman, I. (1991) *Science* **253**, 872–879.
56. Radic, Z., Gibney, G., Kawamoto, S., MacPhee-Quigley, K., Bongiorno, C. & Taylor, P. (1992) *Biochemistry* **31**, 9760–9767.
57. Reiter, M. J., Cowburn, D. A., Prives, J. M. & Karlin, A. (1972) *Proc. Natl. Acad. Sci. USA* **69**, 1168–1172.